Chemical Science

ROYAL SOCIETY OF CHEMISTRY

EDGE ARTICLE

View Article Online
View Journal | View Issue

Cite this: *Chem. Sci.*, 2024, **15**, 14287

All publication charges for this article have been paid for by the Royal Society of Chemistry

Received 29th April 2024
Accepted 2nd August 2024

DOI: 10.1039/d4sc02842b

rsc.li/chemical-science

Manganese catalyzed chemo-selective synthesis of acyl cyclopentenes: a combined experimental and computational investigation†

Koushik Sarkar,[a] Prativa Behera,[b] Lisa Roy *[b] and Biplab Maji *[a]

Cyclopentenes serve as foundational structures in numerous natural products and pharmaceuticals. Consequently, the pursuit of innovative synthetic approaches to complement existing protocols is of paramount importance. In this context, we present a novel synthesis route for acyl cyclopentenes through a cascade reaction involving an acceptorless-dehydrogenative coupling of cyclopropyl methanol with methyl ketone, followed by a radical-initiated ring expansion rearrangement of the *in situ* formed vinyl cyclopropenone intermediate. The reaction, catalyzed by an earth-abundant metal complex, occurs under milder conditions, generating water and hydrogen gas as byproducts. Rigorous control experiments and detailed computational studies were conducted to unravel the underlying mechanism. The observed selectivity is explained by entropy-driven alcohol-assisted hydrogen liberation from an Mn-hydride complex, prevailing over the hydrogenation of unsaturated cyclopentenes.

Introduction

Cyclopentenes are abundant in natural products (Scheme 1a) and are used as pharmaceuticals and medicinal compounds. Because of such importance, the synthesis of cyclopentenes seeks attention.[1–5] Compared to the venerable cyclohexene synthesis *via* the Diels–Alder reaction, the preparation of cyclopentenes *via* [3 + 2] cycloaddition is limited in prominence.[6] The synthesis of cyclopentenes *via* hydrogenation of cyclopentadiene suffers from harsh reaction conditions and poor selectivity due to the uncontrolled over-reduction.[7–9] Other approaches to the synthesis of cyclopentenes *via* ring-closing metathesis needed the synthesis of pre-functionalized alkenes and precious metal catalysts.[10,11] Vinyl cyclopropane rearrangement required multistep starting materials and harsh thermal,[12–14] photochemical,[15,16] or transition metal-catalyzed reaction conditions.[12,16–18] Recently, carbonyl-alkene metathesis[19] and photochemical annulation reactions[6] have also been applied to the synthesis of cyclopentenes. However, the requirement of expensive synthesis of starting materials limits the usefulness of these methodologies. Undoubtedly, intermolecular divergent catalytic protocols utilizing abundant materials are underdeveloped and are in demand to render new retrosynthesis of these families of carbocycles.

Hydrogen transfer (HT) catalysis has become a versatile tool for waste-free redox transformations.[20,21] Not long ago,

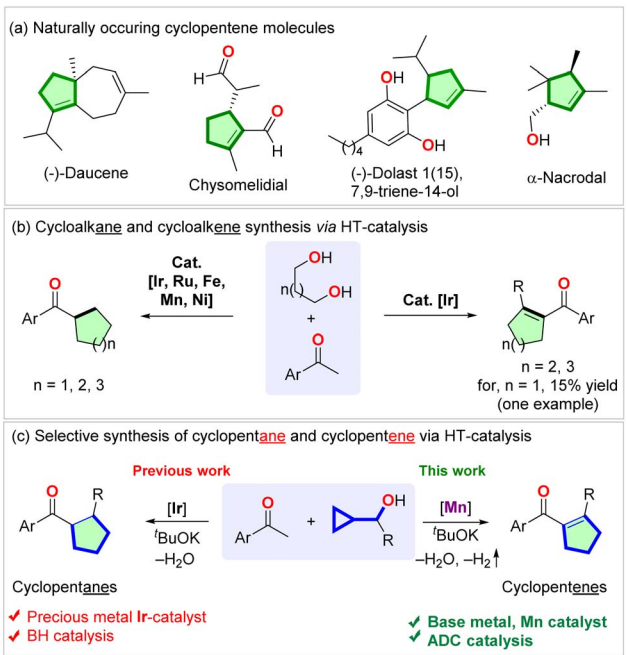

Scheme 1 (a) Selected naturally occurring cyclopentene drug molecules; (b) previous report of the synthesis of cyclopentenes; (c) HT-mediated synthesis of cycloalkanes and cycloalkenes; (d) selective synthesis of cyclopentanes and cyclopentenes *via* HT-catalysis.

[a]*Department of Chemical Sciences, Indian Institute of Science Education and Research Kolkata, Mohanpur, 741246, West Bengal, India. E-mail: bm@iiserkol.ac.in*

[b]*Institute of Chemical Technology Mumbai, IOC Odisha Campus Bhubaneswar, Bhubaneswar, 751013, India. E-mail: l.roy@iocb.ictmumbai.edu.in*

† Electronic supplementary information (ESI) available. CCDC 2237272, 2237255, 2237258, 2237269 and 2376543. For ESI and crystallographic data in CIF or other electronic format see DOI: https://doi.org/10.1039/d4sc02842b

Donohoe, Leitner, Maji, and Adhikary utilized the borrowing hydrogenation (BH) catalysis to synthesize cycloalkanes *via* the annulation of aryl ketones and diols using iridium,[22–24] manganese,[25,26] and nickel[27] catalysts (Scheme 1b, left side). By tuning the ligand and the reaction conditions, the iridium-catalyzed reaction enabled the chemo-selective synthesis of cyclohexenes from pentamethylacetophenone and 1,5-diols (Scheme 1b, right side).[24] However, the same reaction using 1,4-diol gave only 15% yield of one cyclopentene.[24] Recently, Donohoe reported iridium-catalyzed preparation of saturated cyclopentanes (Scheme 1c, left side).[28] However, to our knowledge, the applications of HT catalysis in synthesizing cyclopentenes have not been developed thus far (Scheme 1c, right side).

Employing an earth-abundant metal as a catalyst has an added advantage to sustainable chemical synthesis.[21,29] Manganese complexes have recently been recognized as powerful catalysts for diverse (de)hydrogenation and hydroelementation reactions.[30–32] Particularly, Mn(I)-complexes showed excellent activities in dehydrogenative coupling reactions without needing an acceptor for the liberated hydrogen.[33,34] We are recently intrigued by the possibility of synthesizing multi-substituted acyl cyclopentenes *via* the Mn(I)-complex catalyzed HT-mediated coupling of cyclopropyl methanol with methyl ketone, followed by a single electron transfer (SET)-initiated ring expansion rearrangement of the *in situ* formed vinyl cyclopropenone intermediate (Scheme 1c, right side). We envisioned that by tailoring the catalyst and reaction conditions, it would be possible to facilitate the acceptorless liberation of a hydrogen molecule from a Mn(I)-hydride intermediate before the hydrogenation of the weakly polarized tetrasubstituted alkene could take place. It could thus enable the isolation of these unsaturated compounds, leading to the development of an unprecedented divergent synthesis of cyclopentenes with the generation of water and hydrogen as the byproducts. Herein, we report the realization of the above mechanistic hypothesis. Furthermore, controlled experiments and extensive DFT calculations were performed to understand the reaction mechanism.

Results and discussion

Reaction optimization

We began the project by inquiring about the reaction of pentamethyl acetophenone **1a** and 1-phenyl cyclopropyl methanol **2a** for synthesizing acyl cyclopentene **3a** (Table 1, Section S4†). We realized the unique selectivity issue as the HT-mediated cascade of **1a** and **2a** could, together with the desired cyclopentene **3a**, yield saturated cyclopentane **4a**, BH product **5a**, and unrearranged product **6a**. Upon extensive optimization, we have found that the manganese complex **Mn1** derived from the commercially available ^{Ph}MACHO-ligand produced the desired cyclopentene **3a** in 90% yield in the presence of ^{t}BuOK in toluene at 140 °C (entry 1). While **4a** was undetected, trace amounts of **5a** and **6a** were observed by gas chromatography. The reaction was found to be sensitive to the bifunctional ligands. The Mn(I)-complexes **Mn2,3** derived from ^{iPr}MACHO- and PN_5P-ligands, respectively, provided inferior results (entries

Table 1 Selected reaction optimization[a]

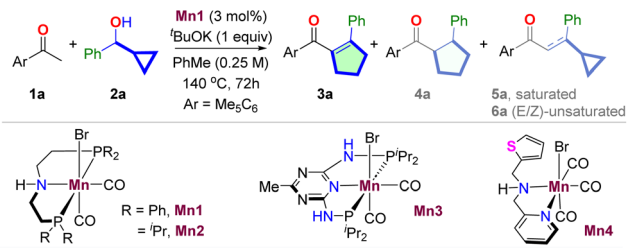

Entry	Deviation from the above	Selectivity **1a** : **3a** : **4a** : **5a** : **6a**	% Yield of **3a**
1	None	2 : 90 : 0 : 5 : 2	90 (75)
2	**Mn2** instead of **Mn1**	5 : 51 : 2 : 3 : 0	51
3	**Mn3** instead of **Mn1**	8 : 57 : 4 : 2 : 0	57
4	**Mn4** instead of **Mn1**	6 : 72 : 22 : 0 : 0	72
5	NaO^{t}Bu instead of KO^{t}Bu	44 : 45 : 0 : 0 : 0	45
6	LiO^{t}Bu instead of KO^{t}Bu	40 : 20 : 0 : 3 : 0	20
7	KOH instead of KO^{t}Bu	55 : 34 : 0 : 2 : 0	34
8	Hexane instead of PhMe	3 : 87 : 4 : 0 : 0	87
9	Dioxane instead of PhMe	4 : 34 : 4 : 0 : 0	34
10	^{t}AmOH instead of PhMe	50 : 4 : 0 : 0	4
11	Without **Mn1**	100 : 0 : 0 : 0 : 0	0
12	Without KO^{t}Bu	100 : 0 : 0 : 0 : 0	0

[a] Reaction conditions: **1a** (0.1 mmol), **2a** (0.2 mmol), Mn-catalyst (3 mol%), ^{t}BuOK (1 equiv.), PhMe (0.4 mL), 140 °C, 72 h. Selectivity and yields were calculated *via* gas chromatography using mesitylene as the internal standard. The poor mass balance in some cases is due to the complex, undetected product mixture. Ar=C_6Me_5.

Table 2 Substrate scope[a]

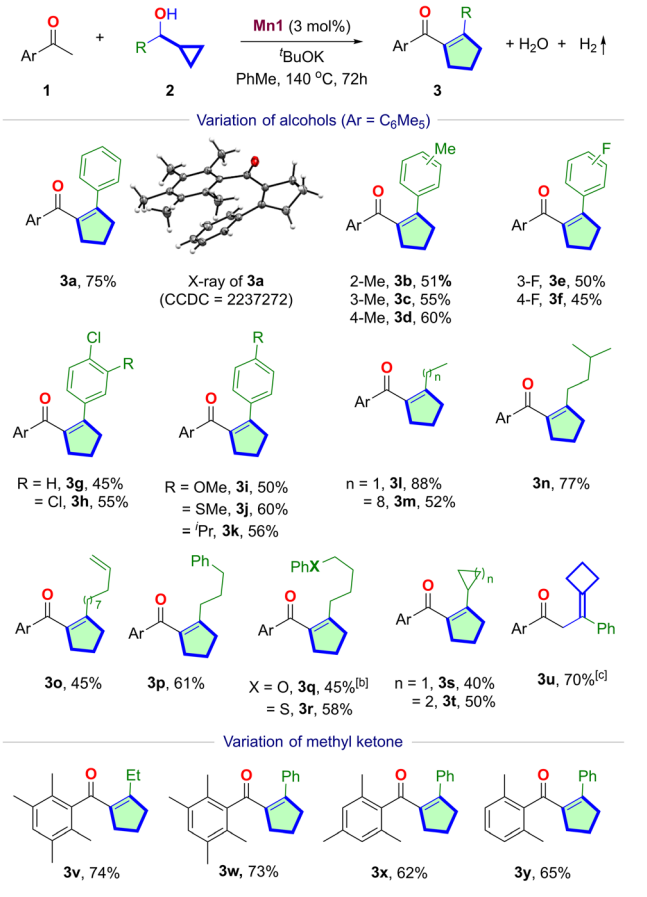

[a] Reaction conditions: ketone (0.1 mmol), alcohol (0.2 mmol), **Mn-1** (3 mol%), tBuOK (1 equiv.), PhMe (0.4 mL), 140 °C, 72 h. Ar=C_6Me_5. [b] 0.8 M toluene. [c] With 1-phenyl cyclobutyl methanol **2'**. 0.8 M toluene and 48 h.

Table 3 Reactions with different cyclopropyl rings[3a]

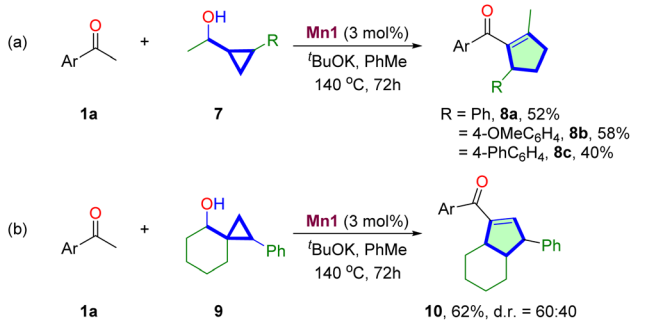

[3a] Reaction conditions: **1a** (0.1 mmol), **7** or **9** (0.2 mmol), Mn-catalyst (3 mol%), tBuOK (1 equiv.), PhMe (0.4 mL), 140 °C, 72 h. Ar=C_6Me_5.

2 and 3). The *N*,*N*-chelated Mn(I)-complexes **Mn4** that we previously used for cycloalkane synthesis also gave poor results (entry 4).[26] A significant amount of cyclopentane **4a** was formed in the later case. The reaction was also sensitive to the bases used (entries 5–7). tBuOK performed better than other bases tested. Among the solvents, *n*-hexane gave a similar efficiency (entry 9), while others provided poor outcomes (entries 9–10). Control experiments suggested the necessity of each reaction component for successful product formation (entries 11–12).

Tolerances of the method

With the set of optimized conditions, we explored the scope of Mn(I)-catalyzed cascade cyclopentene synthesis (Table 2). The reaction was minimally affected by the sterics, as *o*-, *m*-, and *p*-tolyl cyclopropylmethanol reacted with **1a** at similar efficiencies, yielding the desired cyclopentenes **3b–3d** in similar yields. The reaction tolerates halogens at different positions of the aryl ring, delivering **3e–3h** in moderate yields. Aryl cyclopropylmethanol containing *p*-OMe, *p*-SMe, and *p*-^{i}Pr groups also reacted smoothly, providing the cyclopentenes **3i–3k** in 50–60% yields. In particular, the reaction was equally efficient with the more challenging alkyl cyclopropylmethanols **3l–3s**. 1-Cyclopropylpropan-1-ol provided **3l** in 88% yield. While the increase in the chain length (**3m**) slightly lowered the yield, branching (**3n**) imparted minimal influence. A terminal alkene in **3o** is retained under these hydrogen-liberating conditions. Similar observations were made with phenyl, ether, and thioether-containing substrates **3p–3r**. Interestingly, dicyclopropylmethanol can also yield β-cyclopropyl cyclopentene **3s** in a moderate 40% yield. Similarly, β-cyclobutyl cyclopentene **3t** was synthesized in 50% yield. However, for the 1-phenyl cyclobutyl methanol, we obtained an exocyclic cylobutyl alkene product **3u**, with 70% yield (Section S4.9†). The structures of **3a** and **3u** were confirmed *via* single-crystal X-ray crystallography.

Diverse *ortho*-disubstituted acetophenones can be utilized as the C1-units yielding cyclopentenes **3v–3y** in 62–74% yields. However, when **2a** was treated with acetophenone under standard conditions, a complex mixture resulted, indicating the necessity of *ortho*-substituents that can sterically shield the carbonyl group to slow down reduction and aldol condensations. The advantageous effect of *ortho*-disubstituted methyl ketone has previously been demonstrated.[22]

Then, we were prompted to explore the scope of substituted cyclopropane methanols for synthesizing multisubstituted cyclopentenes (Table 3). The reactions of 1,2-disubstituted cyclopropane methanols **7** with **1a** proceed smoothly to produce 1,2,3-trisubstituted cyclopentenes **8a–8c** in moderate 40–58% yields. The reaction of spiro-bicyclic cyclopropyl alcohol **9** was also investigated. The reaction proceeds at a similar efficiency, producing ring-expanded bicyclic product **10** in 62% yield, albeit in moderate 60 : 40 d.r.

Synthetic utility

To explore the synthetic utility of the Mn(I)-catalyzed cascade reaction, we have performed derivatization of isolated cyclopentene products (Scheme 2). The Pd/C catalyzed hydrogenation of **3a** and produced the saturated carbocycle **11** in 70% yield. Corey–Chaykovsky cyclopropanation of **3l** delivered bicyclo[3.1.0]hexan-1-yl core **12** in 62% yield and >99 : 1 d.r. We have also conducted the epoxidation of **3l**. The reaction with tBuOOH/NaOH produced the tetra-substituted bicyclic epoxide

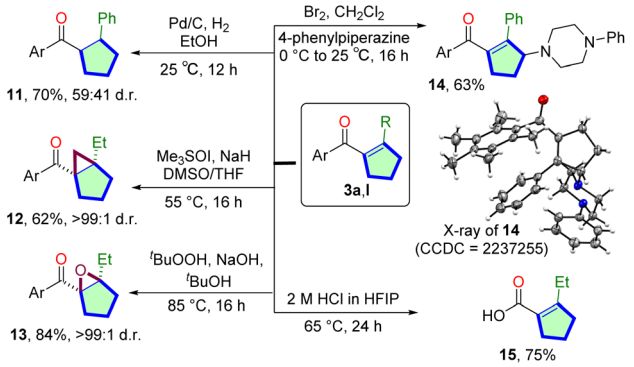

Scheme 2 Derivatization of the product.

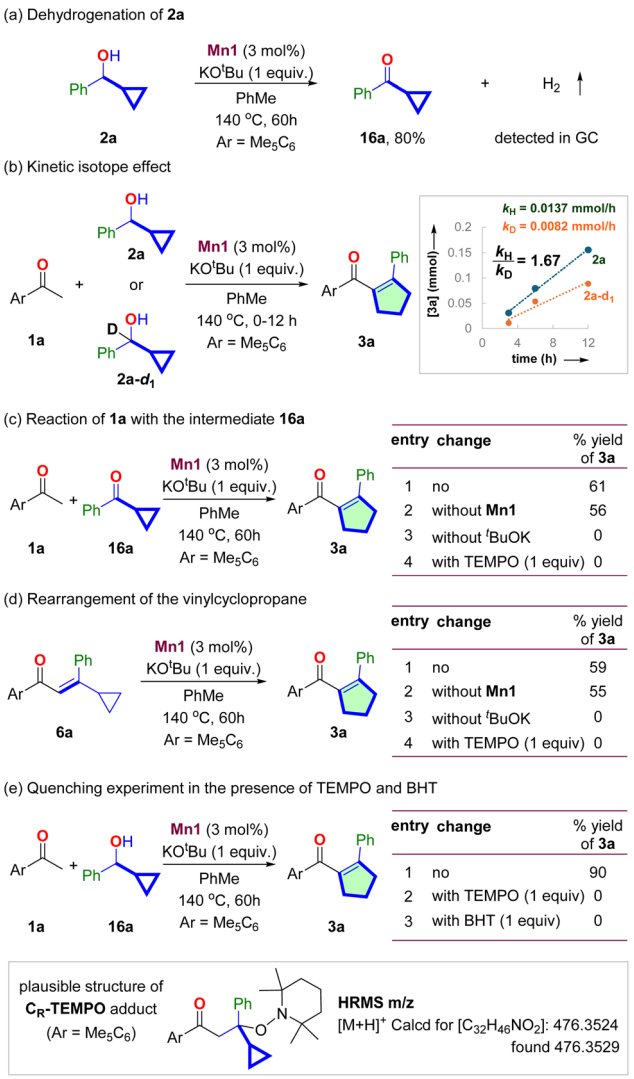

entry	change	% yield of 3a
1	no	61
2	without **Mn1**	56
3	without ^{t}BuOK	0
4	with TEMPO (1 equiv)	0

entry	change	% yield of 3a
1	no	59
2	without **Mn1**	55
3	without ^{t}BuOK	0
4	with TEMPO (1 equiv)	0

entry	change	% yield of 3a
1	no	90
2	with TEMPO (1 equiv)	0
3	with BHT (1 equiv)	0

Scheme 3 Mechanistic studies. (a) Dehydrogenation of **2a**, (b) kinetic isotope effect study, (c) reaction of **1a** with **16a**, (d) probing the intermediacy of vinyl cyclopropane, (e) probing the involvement of radicals and plausible structure of the TEMPO adduct.

13 in a high 84% yield with >99 : 1 d.r. To further functionalize the product, we have performed late-stage γ-amination of **3a** *via* bromine treatment in the presence of piperazine. Allyl amine **14** was isolated in 63% yield. The molecular structure of **14** was confirmed *via* single-crystal X-ray crystallography.[35] Finally, the pentamethyl aryl group can easily be deprotected *via* retro-Friedel–Craft reactions. The free cyclopentene-1-carboxylic acid **15** was isolated in 75% yield.

Mechanistic studies and proposed mechanism

The **Mn1**-catalyzed dehydrogenation of **2a** in the absence of **1a** produced the corresponding ketone **16a** in 80% yield (Scheme 3a, see Section S7.1†). The reaction proceeded without an acceptor, and hydrogen gas was detected upon GC analysis of the reaction headspace. The deuterium kinetic isotope effect experiment with **2a** and **2a-*d*$_1$** shows $k_H/k_D = 1.67$ (Scheme 3b, see Section S7.2†). It indicated that the dehydrogenation of secondary cyclopropyl alcohol could be the slowest step of the catalytic cycle. The reaction of **16a** with **1a** under the standard conditions gave 61% yield of product **3a** (Scheme 3c, see Section S7.3†). The same reaction without **Mn1** also gave a similar yield of **3a**. However, no reaction occurred in the absence of ^{t}BuOK. It confirms the intermediacy of **16a** and highlights the necessity of the base for the condensation and rearrangement steps.

We then synthesized the vinyl cyclopropane **6a** and performed control experiments to probe its intermediacy (Scheme 3d, Section S7.4†). The subjection of **6a** under standard conditions resulted in 59% yield of **3a** (Scheme 3b, entry 1). The same reaction without **Mn1** also provided 55% yield of **3a** (entry 2). However, in the absence of ^{t}BuOK, **3a** did not form, and 70% of **6a** was recovered as an *E*/*Z* mixture (entry 3). These experiments suggested that (i) **6a** is an intermediate for this reaction. (ii) Thermal vinyl-cyclopropane rearrangement did not occur at the reaction temperature. (iii) ^{t}BuOK mediates the rearrangement of **6a** to **3a**.

Notably, the isomerization of **6a** to **3a** stops in the presence of known radical quenchers, such as 2,2,6,6-tetramethylpiperidine 1-oxyl (TEMPO) (entry 4). The reaction of **1a** with **2a** in the presence of TEMPO and butylated hydroxytoluene (BHT) also did not produce **3a** (Scheme 3e, see Section 7.5†). A similar observation was also made for the reaction of **16a** with **1a** (Scheme 3c, entry 4). High-resolution mass spectrometric analysis of the reaction mixture detected $m/z = 476.3529$, corresponding to a TEMPO adduct with the composition $[C_{32}H_{45}NO_2]$, suggesting the involvement of radical species during the rearrangement step (Scheme 3e).

The studied reaction holds promise for an intriguing ring expansion cascade. To provide in-depth insights into the reaction mechanism, we have further investigated the reaction using density functional theory at B3LYP-D3(BJ)/SMD(toluene)/def2-TZVPP (Fig. 1, 2, and Section S8†). For simplicity, we have bifurcated the reaction into (a) Mn-catalyzed dehydrogenation (Fig. 1a and b show the reaction mechanism and corresponding energy profile, respectively) and (b) the aldol condensation coupled to the SET cascade rearrangement (Fig. 2 shows the energy profile and structures of stationary states).

We began by investigating the proposed catalytic cycle for the **Mn1**-catalyzed dehydrogenation of alcohol **2a** to ketone **16a** (Fig. 1a). As anticipated, our computational studies indicate

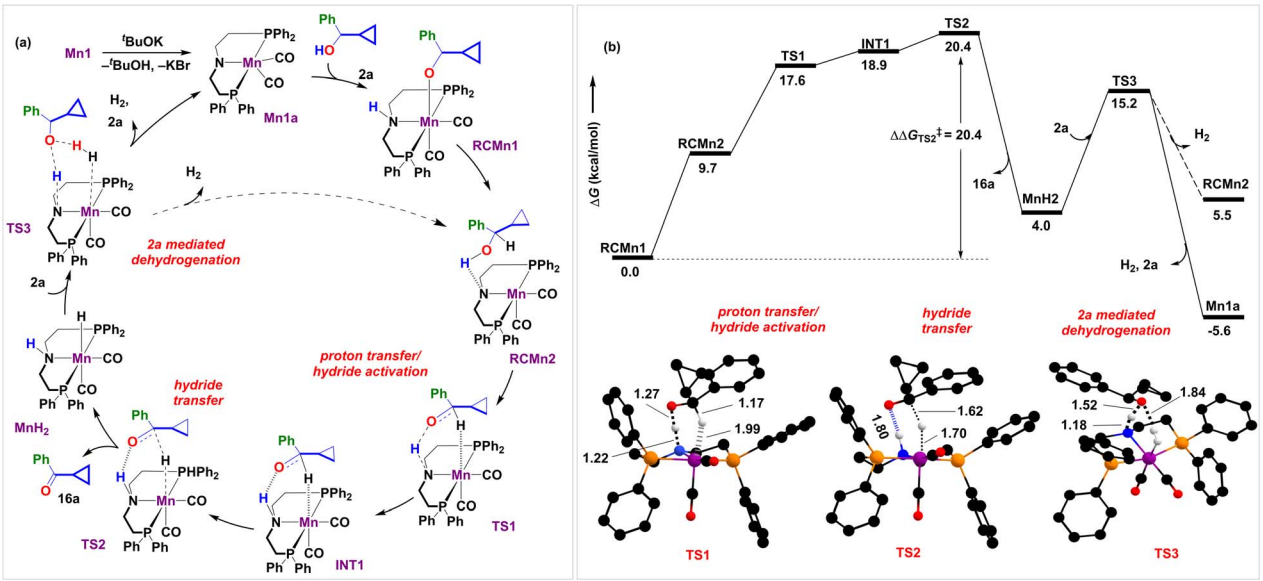

Fig. 1 (a) Proposed mechanism for the **Mn1**-catalyzed dehydrogenation of **2a** and (b) the corresponding reaction free energy profile at B3LYP-D3(BJ)/SMD(toluene)/def2-TZVPP (in kcal mol^{-1}) for the Mn catalyzed dehydrogenation of alcohol. Color coding for optimized geometries (truncated) **TS1**, **TS2**, **TS3**: C(black), H(white), O(red), P(orange), N(blue), Mn(purple). Distances shown are in units of Å. Unimportant hydrogen atoms are not shown for clarity.

that the high spin quintet (28.8 kcal mol^{-1}) and the intermediate spin triplet (26.0 kcal mol^{-1}) of the octahedral complex **Mn1** are high in energy as compared to the singlet ground-state complex. Thus, we have considered all singlet state structures to compute the catalytic cycle. In the presence of an external base, the complex **Mn1** undergoes dehydrobromination to give the catalytically active amido complex **Mn1a** (Fig. 1a), reported earlier as a penta-coordinate intermediate in analogous **Mn**

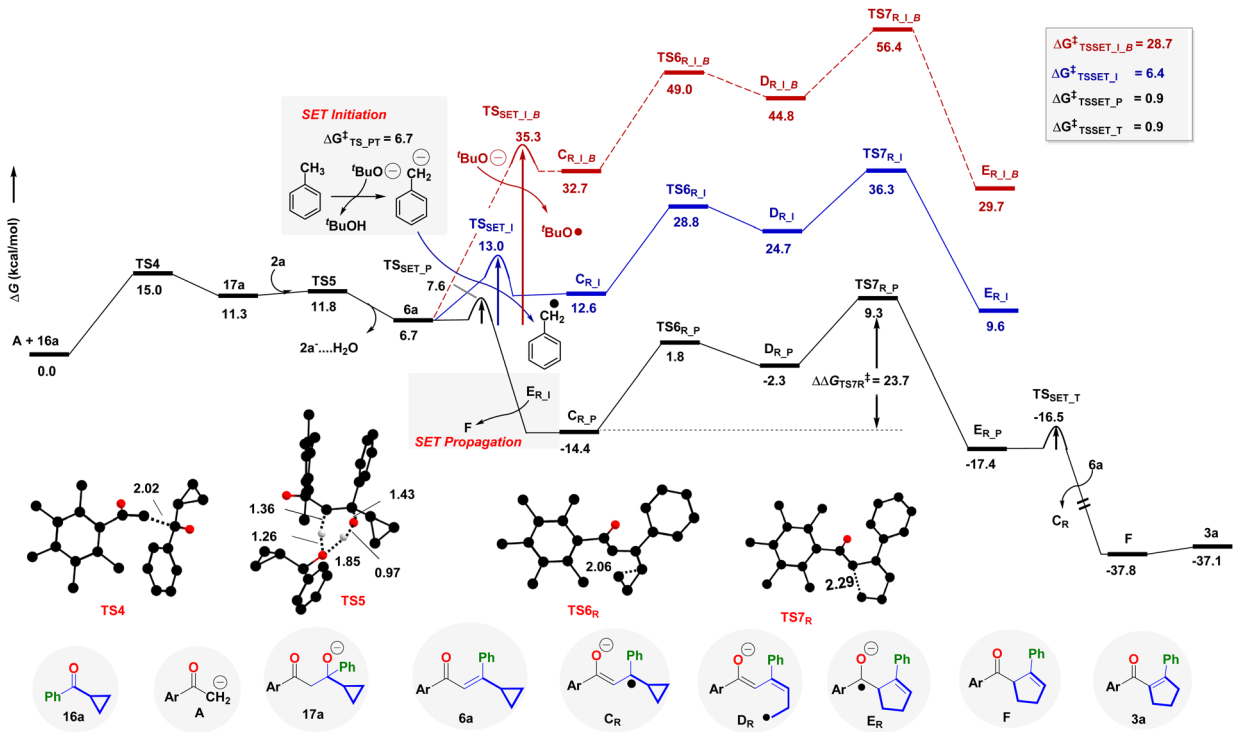

Fig. 2 Reaction free energy profile at B3LYP-D3(BJ)/SMD(toluene)/def2-TZVPP (in kcal mol^{-1}) for the synthesis of cyclopentene **3a**. Color coding for optimized geometries (truncated) **TS4**, **TS5**, **TS6$_R$**, **TS7$_R$**: C(black), H(white), O(red), P(orange), N(blue), Mn(purple). Distances shown are in units of Å. Unimportant hydrogen atoms are not shown for clarity.

complexes on treatment with ^{t}BuOK.[36] We have recently characterized **Mn1a**.[37] Similar pre-activation of the catalyst has been crucial to facilitate substrate binding, as observed by us and others.[38,39] Indeed, adding alcohol **2a** to **Mn1a** results in a computationally identified octahedral reactant complex, **RCMn1** ($\Delta G = -9.9$ kcal mol^{-1}). Here, the alcoholic O–H bond is activated by the Mn–N framework, leading to the alkoxide coordination with the metal and protonation of the amido group. A similar resting state has been identified by Gauvin and others in acceptorless dehydrogenation of ethanol by the analogous **Mn2** complex employing multinuclear NMR spectroscopy.[40,41] In congruence with previous reports,[40–44] we hypothesize that the catalytic cycle consists of three crucial steps: proton transfer/hydride activation, hydride transfer, and **2a** alcohol mediated H_2 release. Next to **RCMn1**, an adduct **RCMn2** is hypothesized that shows strong N···H–O interaction and initiates metal–hydride interaction. This triggers a reversal proton transfer between the hydroxyl and the amido groups, complemented with hydride activation at 1.17 Å in **TS1**.[40] In fact, this has been validated by intrinsic reaction coordinate scans (see Fig. S6†). This is a facile process with an intrinsic energetic cost of 7.9 kcal mol^{-1}, generating **INT1** in an endergonic manner. Next is the crucial β-hydride elimination through **TS2** at a moderate barrier ($\Delta G^{\ddagger} = 20.4$ kcal mol^{-1}). However, the ^{t}BuOK-mediated dehydrogenation of **2a** required a 29 kcal per mol barrier. A similar dehydrogenation of alcohol is a rather difficult process by a Ni–phenanthroline complex, as observed by one of us,[45,46] presumably due to the absence of strong O^{-}···H–N hydrogen bonding in **TS2**, emphasizing on the crucial role of the N–H bifunctionality in the MACHO ligand of **Mn1**. In fact, Fu *et al.* have reported lowered reactivity of *N*-methyl substituted analogous Mn complexes in upgradation of ethanol.[41] **TS2** is succeeded by releasing the ketone **16a** and forming an Mn(I)-H intermediate **MnH_2**. The process is slightly endergonic (~4.0 kcal mol^{-1}). We have previously identified similar Mn(I)-alkoxy (**RCMn1**) and Mn(I)-hydride (**MnH_2**) complexes *via* NMR experiments.[47] The ketone **16a** further participates in a separate aldol condensation reaction (*vide infra*).

Experimentally, H_2 gas evolution was confirmed through gas chromatographic analysis of the reaction headspace (see Sections S7.1 and S7.8†). The development of partial hydride and protic characters on hydrogen atoms over Mn and N in **MnH_2** is hypothesized to trigger the release of H_2 (Fig. 1a). This can occur either through an inner-sphere self-dehydrogenation process[46] when the N–H proton couples to the Mn–H hydride (Fig. 3 and S5†) or through an outer-sphere concerted proton-relay mechanism involving an alcohol **2a** (Fig. 1 and 3).[41,48] Out of the two possibilities, the former overcomes a higher intrinsic barrier ($\Delta\Delta G^{\ddagger} = 24.3$ kcal mol^{-1}, *via* **$TS3_{self}$**, Fig. 3b) than the latter ($\Delta\Delta G^{\ddagger} = 11.1$ kcal mol^{-1}, *via* **TS3**, Fig. 3b) concerning the reference state, **MnH_2**, suggesting that H_2 evolution would be kinetically feasible on treatment with **2a**. Interestingly, the stronger H–H interaction at 0.79 Å in **TS3** as compared to 0.91 Å in **$TS3_{self}$** might be responsible for the observed role of alcohol in facilitating the dehydrogenation process (see Section S8.4†).[48]

The aldol condensation of **1a** and **16a** to the enone **6a** proceeds *via* the intermediacy of **17a** (Fig. 2, Section S8†). The base ^{t}BuO^{-} initiates the reaction through **TS4** at 15.0 kcal mol^{-1} kinetic barrier; whereas alcohol **2a** helps in the dehydration *via* **TS5** at $\Delta G^{\ddagger} = 11.8$ kcal mol^{-1}. However, dehydration through

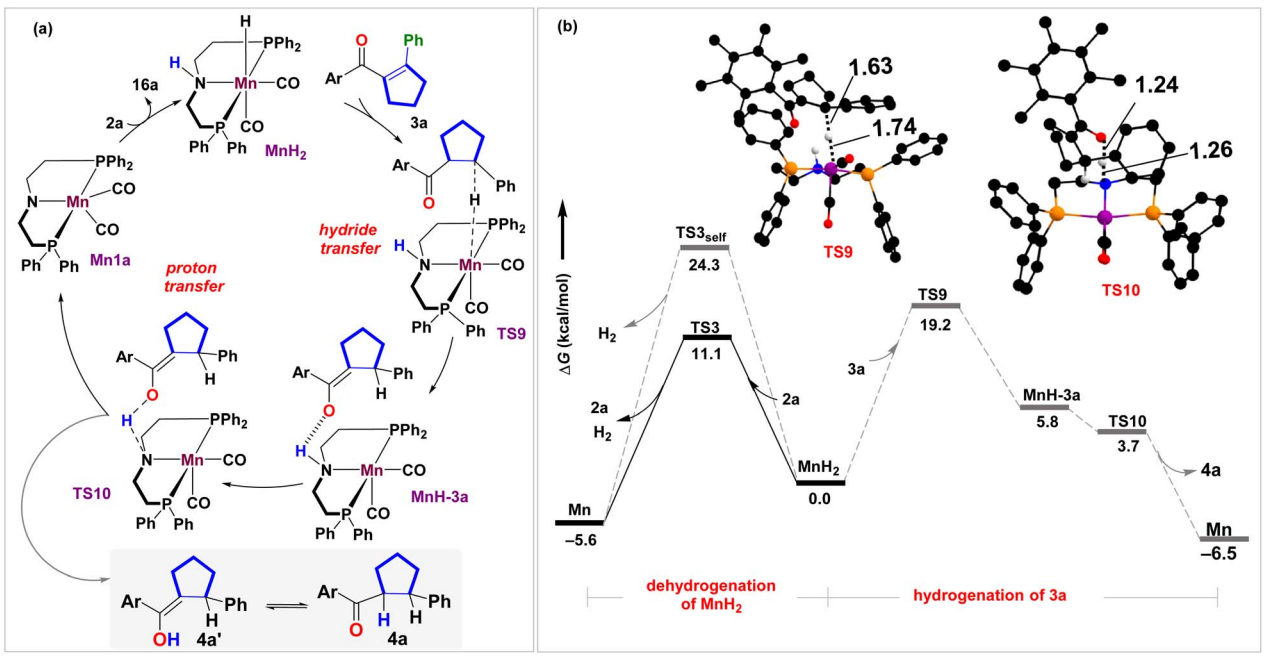

Fig. 3 (a) Reaction mechanism and (b) corresponding free energy profile at B3LYP-D3(BJ)/SMD(toluene)/def2-TZVPP (in kcal mol^{-1}) for the hydrogenation of cyclopentene **3a**. Color coding for optimized geometries (truncated) **TS9**, **TS10**: C(black), H(white), O(red), P(orange), N(blue), Mn(purple). Distances shown are in units of Å. Unimportant hydrogen atoms are not shown for clarity.

the intermediacy of ^{t}BuOH is sluggish at $\Delta G^{\ddagger} = 14.7$ kcal mol^{-1}. At this stage, we have explored different possibilities for rearranging **6a** to **3a**, either through radical mediation or nucleophilic attack (Fig. 2, see Section S8† for details). The ^{t}BuO$^-$ mediated SET initiation pathway required a 28.7 kcal mol^{-1} energetic requirement (**TS$_{SET_I_B}$**, Fig. 2 and S4†). We identify that ^{t}BuO$^-$ could execute the deprotonation of an explicit solvent molecule ($\Delta G^{\ddagger} = 6.7$ kcal mol^{-1}) that results in the generation of the tolyl anion that could facilitate the initiation process on **6a** at a SET barrier of 6.4 kcal mol^{-1} (**TS$_{SET_I}$**, Fig. 2). Thus, the SET transforms enone **6a** to the enolate radical **C$_R$** in an endoergic fashion. Once **C$_R$** is formed, it undergoes a stepwise ring opening and ring closer rearrangement process through **TS6$_R$** and **TS7$_R$**, to deliver the enone radical anion **E$_R$**, with the intermediacy of the transient radical species **D$_R$**. Notably, the radical initiation with the tolyl anion affords the effective barriers of **TS6$_R$** and **TS7$_R$** as 28.8 and 36.3 kcal mol^{-1}, respectively. This is totally in agreement with the high temperature (140 °C) requirement.

However, once **E$_R$** is produced *in situ*, it significantly curtails down the kinetic barrier for SET to 0.9 kcal mol^{-1}, as well as stabilizing the radical anion intermediate **C$_R$** as referenced with **6a** (Fig. 2). Hence, the radical chain propagation by an electron transfer from **E$_R$** transforms **6a** to **C$_R$** and furnishes the required driving force to develop a β,γ-unsaturated 5-membered cyclopentene **F** during the radical chain termination. This is the reason the radical propagation steps, as shown by the black lines in Fig. 2, display a lower transition state barrier **TS7$_R$** (23.7 kcal mol^{-1}) and overall exothermicity. Thereby, isomerism of **F** leads to the targeted α,β-unsaturated cyclopentene product **3a**. Our study also unfurls the unique role of catalytic electrons in novel cascade reactions and augments the chemical space with the already rich literature on efficient electron-catalyzed reactions.[49]

Once we reach product molecule **3a**, one may fathom **MnH$_2$**-mediated hydrogenation of the cyclopentene ring to the saturated product **4a** (Fig. 3 and S5†), as observed previously with the [Ir(cod)Cl]$_2$/cataCXiumA catalyst.[28] Here, we propose a stepwise hydride/proton transfer to β-C and carbonyl O-centers, respectively, to generate the corresponding enol intermediate **4a′**, which gets interconverted to **4a**. To initiate the hydrogenation process, **3a** binds to **MnH$_2$** through weak C=O···H–N intermolecular H-bonding in **TS9** (Fig. 3 and S5†), which catalyzes the initial Mn → C(β) hydride transfer at an energetic barrier of 19.2 kcal mol^{-1} followed by a relatively stable intermediate, **MnH-3a**. The consequent proton transfer step occurs (**TS10**) at a low energetic requirement to generate the target cyclopentane in an exoergic fashion. Essentially, under the experimental conditions, the transfer hydrogenation cascade mechanism is possible. However, a closer inspection reveals that the alcohol-mediated dehydrogenation of **MnH$_2$** is kinetically more facile ($\Delta\Delta G^{\ddagger} = 11.1$ kcal mol^{-1}, *via* **TS3**) than hydrogenation of **3a** ($\Delta\Delta G^{\ddagger} = 19.2$ kcal mol^{-1}, *via* **TS9**). The competitive H$_2$ release mechanism should be favorable entropically and thus rationalize the observation of an unsaturated cyclopentene product **3a** (see Section S8.3†).

Conclusion

We reported the first example of the synthesis of acyl cyclopentenes *via* coupling cyclopropane methanol and aryl methyl ketones. A manganese complex derived from a commercially available ligand catalyzed the reaction, delivering the products in moderate to high yields with good selectivities. Water and hydrogen gas were produced as the byproducts. The detailed experimental and computational studies elucidated the reaction mechanism that involved multistep manganese-catalyzed acceptorless alcohol dehydrogenation, aldol condensation, and SET-mediated vinyl cyclopropane ring expansion. Facile alcohol-assisted hydrogen liberation over the hydrogenation of enones explains the selectivity for cyclopentene products. Further, we propose an uncharted mechanism of cooperativity between metal/single electron catalysis that we believe could inspire the design of new cascade reactions.

Data availability

The ESI† includes all experimental details, including optimization of the synthetic method, synthesis, and characterization of all starting materials and products reported in this study, and mechanistic studies. NMR spectra of all products, crystallography, and computation details are included as well.

Author contributions

KS and BM conceived the project. KS performed experiments, analyzed products, and performed experimental mechanistic studies with input from BM. PB performed the DFT calculations with input from LR. KS and PB wrote the initial draft with input from BM and LR. BM and LR edited the manuscript. BM and LR acquired financial support for the development of this project.

Conflicts of interest

The authors declare no conflict of interest.

Acknowledgements

BM thanks IISER Kolkata and CSIR 02(0405)/21/EMR-II for financial support. LR thanks SERB, India (SPG/2020/000754) for funding. KS and PB thank CSIR and ICT-IOCB, respectively, for PhD fellowships.

References

1 M. Ansell, *Supplements to the 2nd Edition of Rodd's Chemistry of Carbon Compounds. A Modern Comprehensive Treatise*, 2008.
2 J. Meinwald and T. H. Jones, *J. Am. Chem. Soc.*, 1978, **100**, 1883–1886.
3 K. M. Daane, G. Y. Yokota, V. M. Walton, B. N. Hogg, M. L. Cooper, W. J. Bentley and J. G. Millar, *Insects*, 2020, **11**, 635.

4 A. J. Ferreira and C. M. Beaudry, *Tetrahedron*, 2017, **73**, 965–1084.
5 J.-B. Sortais, R. Buhaibeh and Y. Canac, in *Manganese Catalysis in Organic Synthesis*, ed. S. Jean-Baptiste, Wiley-VCH, Weinheim, 2021, pp. 39–66, DOI: 10.1002/9783527826131.ch2.
6 F. J. Sarabia, Q. Li and E. M. Ferreira, *Angew. Chem., Int. Ed.*, 2018, **57**, 11015–11019.
7 Y.-S. Feng, J. Hao, W.-W. Liu, Y.-J. Yao, Y. Cheng and H.-J. Xu, *Chin. Chem. Lett.*, 2015, **26**, 709–713.
8 H. Gao, Y. Xu, S. Liao, R. Liu, J. Liu, D. Li, D. Yu, Y. Zhao, Y. Fan and J. Memdr, *Science*, 1995, **106**, 213–219.
9 C. Liu, Y. Xu, S. Liao and D. Yu, *J. Mol. Catal. A*, 2000, **157**, 253–259.
10 G. Domínguez and J. Pérez-Castells, *Chem.–Eur. J.*, 2016, **22**, 6720–6739.
11 O. M. Ogba, N. C. Warner, D. J. O'Leary and R. H. Grubbs, *Chem. Soc. Rev.*, 2018, **47**, 4510–4544.
12 J. E. Baldwin, *Chem. Rev.*, 2003, **103**, 1197–1212.
13 Z. Goldschmidt and B. Crammer, *Chem. Soc. Rev.*, 1988, **17**, 229–267.
14 C. G. Overberger and A. E. Borchert, *J. Am. Chem. Soc.*, 1960, **82**, 1007–1008.
15 J. J. Li, in *Name Reactions: A Collection of Detailed Reaction Mechanisms*, Springer Berlin Heidelberg, Berlin, Heidelberg, 2006, pp. 606–607.
16 D. Armesto, A. Ramos, E. P. Mayoral, M. J. Ortiz and A. R. Agarrabeitia, *Org. Lett.*, 2000, **2**, 183–186.
17 R. I. Khusnutdinov and U. M. Dzhemilev, *J. Organomet. Chem.*, 1994, **471**, 1–18.
18 M. Rubin, M. Rubina and V. Gevorgyan, *Chem. Rev.*, 2007, **107**, 3117–3179.
19 H. Albright, A. J. Davis, J. L. Gomez-Lopez, H. L. Vonesh, P. K. Quach, T. H. Lambert and C. S. Schindler, *Chem. Rev.*, 2021, **121**, 9359–9406.
20 J. M. Ketcham, I. Shin, T. P. Montgomery and M. J. Krische, *Angew. Chem., Int. Ed.*, 2014, **53**, 9142–9150.
21 K. Das, M. K. Barman and B. Maji, *Chem. Commun.*, 2021, **57**, 8534–8549.
22 R. J. Armstrong, W. M. Akhtar, J. R. Frost, K. E. Christensen, N. G. Stevenson and T. J. Donohoe, *Tetrahedron*, 2019, **75**, 130680.
23 R. J. Armstrong and T. J. Donohoe, *Tetrahedron Lett.*, 2021, **74**, 153151.
24 L. B. Smith, R. J. Armstrong, D. Matheau-Raven and T. J. Donohoe, *J. Am. Chem. Soc.*, 2020, **142**, 2514–2523.
25 A. Kaithal, L.-L. Gracia, C. Camp, E. A. Quadrelli and W. Leitner, *J. Am. Chem. Soc.*, 2019, **141**, 17487–17492.
26 A. Jana, K. Das, A. Kundu, P. R. Thorve, D. Adhikari and B. Maji, *ACS Catal.*, 2020, **10**, 2615–2626.
27 A. K. Bains, A. Kundu, D. Maiti and D. Adhikari, *Chem. Sci.*, 2021, **12**, 14217–14223.
28 S. Wübbolt, C. B. Cheong, J. R. Frost, K. E. Christensen and T. J. Donohoe, *Angew. Chem., Int. Ed.*, 2020, **59**, 11339–11344.
29 Y. Cai, F. Li, Y.-Q. Li, W. Zhang, F.-H. Liu and S. L. J. T. L. Shi, *Tetrahedron Lett.*, 2018, **59**, 1073–1079.
30 K. Das, S. Waiba, A. Jana and B. Maji, *Chem. Soc. Rev.*, 2022, **51**, 4386–4464.
31 G. E. Dobereiner and R. H. Crabtree, *Chem. Rev.*, 2010, **110**, 681–703.
32 Y. Wang, M. Wang, Y. Li and Q. Liu, *Chem*, 2021, **7**, 1180–1223.
33 S. Waiba and B. Maji, *ChemCatChem*, 2020, **12**, 1891–1902.
34 M. K. Barman, S. Waiba and B. Maji, *Angew. Chem., Int. Ed.*, 2018, **130**, 9264.
35 CCDC 2237272 (**3a**), 2237255 (14), 2237258 (**6a**), 2237269† (**5a**), and 2376543 (**3u**) contain the supplementary crystallographic data.
36 Y. Wang, L. Zhu, Z. Shao, G. Li, Y. Lan and Q. Liu, *J. Am. Chem. Soc.*, 2019, **141**, 17337–17349.
37 S. Waiba, K. Maji, M. Maiti and B. Maji, *Angew. Chem., Int. Ed.*, 2023, **62**, e202218329.
38 J. A. Luque-Urrutia, T. Pèlachs, M. Solà and A. Poater, *ACS Catal.*, 2021, **11**, 6155–6161.
39 K. Sarkar, K. Das, A. Kundu, D. Adhikari and B. Maji, *ACS Catal.*, 2021, **11**, 2786–2794.
40 D. H. Nguyen, X. Trivelli, F. Capet, J.-F. Paul, F. Dumeignil and R. M. Gauvin, *ACS Catal.*, 2017, **7**, 2022–2032.
41 S. Fu, Z. Shao, Y. Wang and Q. Liu, *J. Am. Chem. Soc.*, 2017, **139**, 11941–11948.
42 J. A. Luque-Urrutia, T. Pèlachs, M. Solà and A. Poater, *ACS Catal.*, 2021, **11**, 6155–6161.
43 L. M. Azofra and L. Cavallo, *Theor. Chem. Acc.*, 2019, **138**, 64.
44 W. M. Dagnaw, Y. Lu, R. Zhao and Z.-X. Wang, *Organometallics*, 2019, **38**, 3590–3601.
45 V. Arun, L. Roy and S. De Sarkar, *Chem.–Eur. J.*, 2020, **26**, 16649–16654.
46 L. Roy and A. Paul, *Chem. Commun.*, 2015, **51**, 10532–10535.
47 S. Waiba, M. Maiti and B. Maji, *ACS Catal.*, 2022, **12**, 3995–4001.
48 V. Zubar, Y. Lebedev, L. M. Azofra, L. Cavallo, O. El-Sepelgy and M. Rueping, *Angew. Chem., Int. Ed.*, 2018, **57**, 13439–13443.
49 A. Studer and D. P. Curran, *Nat. Chem.*, 2014, **6**, 765–773.